AIAA JOURNAL
Vol. 32, No. 6, June 1994

Three-Dimensional Shape Optimization Using the Boundary Element Method

Koetsu Yamazaki,* Jiro Sakamoto,† and Masami Kitano‡
Kanazawa University, Kanazawa 920, Japan

A practical design sensitivity calculation technique of displacements and stresses for three-dimensional bodies based on the direct differentiation method of discrete boundary integral equations is formulated in detail. Then the sensitivity calculation technique is applied to determine optimum shapes of minimum weight subjected to stress constraints, where an approximated subproblem is constructed repeatedly and solved sequentially by the mathematical programming method. The shape optimization technique suggested here is applied to determine optimum shapes of a cavity in a cube and a connecting rod.

Introduction

THE shape optimization technique using the boundary element method (BEM) has made much progress in recent research[1-6] that was motivated by the advantage that the BEM can analyze the boundary values more precisely than the finite element analysis and that the mesh generation and remeshing are relatively straightforward and inexpensive. For the efficient implementation of the shape optimization in the practical use of large-scale structures, an effective and exact sensitivity analysis and a good approximation method are required to reduce the iteration of the mathematical programming procedure and the structural analysis. Considerable effort has been devoted to developing efficient design sensitivity analysis techniques.[2,4,7-11] These techniques are classified into the direct differentiation method of the discretized integral equation[7-11] and the adjoint variable method.[1,2,4] Mota Soares et al.[1] and Choi and Kwak[2] used a BEM analyzer in generating optimum shapes for planar elastic regions. In their cases, displacement and stress sensitivities were obtained using similar BEM adaptations of the adjoint variable method. Although their approach had already proven successful in the finite element applications, the BEM version was less satisfactory because the approximate adjoint tractions could not be specified uniquely. To overcome this limitation, an alternative to the adjoint variable method was introduced by Barone and Yang.[7] In their formulation, new recovery equations for the design sensitivities were obtained by the direct analytic differentiation of the primitive boundary integral equations for the displacements and the stresses. They have also expanded their formulation to the three-dimensional problem.[9] Another direct approach for determining the design sensitivities has been developed by Kane and Saigal,[8] where the displacement sensitivities were obtained by the implicit differentiation of the coefficient matrices formed by the discretized boundary integral equation and applied to the substructured problems.[11] Most of these studies, however, have treated the two-dimensional elastic bodies, the implicit differentiation formulation of the three-dimensional sensitivity analysis suggested by Kane and Saigal is conceptual, and practical formulation necessary for programming is not provided.

For the efficient implementation of the optimization, a good approximation method as well as an exact sensitivity analysis is also useful to reduce the iterations of the structural analysis and its sensitivity analysis. The Taylor series approximation has been used to form approximate subproblems to the actual design problem. In 1976, Schmit and Miura[12] originally suggested the use of reciprocal variables that can form a wide range approximation for the frameworks. Since then, the reciprocal variable Taylor series approximation has been used widely and has yielded effective results for the frameworks, plates, and shells. Starnes and Haftka[13] and Fleury and Braibant[14] have shown that a hybrid constraint using mixed variables yields a more conservative approximation. Vanderplaats and Salajegheh[15] have suggested, for stress constraints, to use a Taylor series to approximate the internal loads instead of the stresses themselves. Recently, Yang and Botkin[16] and Kodiyalam and Vanderplaats[17] have applied the approximation concepts to the three-dimensional shape optimization using the finite element method. Nevertheless, these approximation techniques have never been applied to the shape optimization process based on the boundary element method.

In this paper, therefore, a practical design sensitivity calculation technique of displacements and stresses for three-dimensional bodies based on the implicit differentiation method of discrete boundary integral equations[9] necessary for programming is formulated in detail, where the stress recovery equation generated by differentiating the standard formula for the boundary stress is adopted. Then the sensitivity calculation technique is applied to determine optimum shapes of minimum weight subjected to stress constraints, where an approximated subproblem formed by the second-order approximated objective function and the first-order approximated stress constraints is constructed repeatedly and solved sequentially by the mathematical programming method. The shape optimization technique suggested here is applied to determine optimum shapes of a cavity in a cube under uniform triaxial tension and a connecting rod under axial compression. From the numerical results, the validity of the technique is discussed.

Three-Dimensional Shape Optimization Problems

Minimum Weight Design Problem

A minimum weight design subject to stress constraints is one of the most important problems in the shape design problems for practical use. Consider the minimum weight design of a three-dimensional body occupying a region Ω with a boundary Γ as shown in Fig. 1. When the shape design

Received March 27, 1993; presented as Paper 93-1642 at the AIAA/ASME/ASCE/AHS/ASC 34th Structures, Structural Dynamics, and Materials Conference, La Jolla, CA, April 19-21, 1993; revision received Dec. 10, 1993; accepted for publication Dec. 13, 1993.

*Associate Professor, Department of Mechanical Systems Engineering, 2-40-20 Kodatsuno. Member AIAA.

†Assistant Professor, Department of Mechanical Systems Engineering, 2-40-20 Kodatsuno. Member AIAA.

‡Graduate Student, Department of Mechanical Systems Engineering, 2-40-20 Kodatsuno.

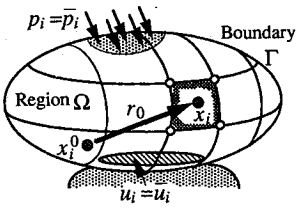

Fig. 1 Shape optimization model.

parameters that describe a boundary shape are taken as the design variables,

$$\boldsymbol{b} = (b_1, b_2, \ldots, b_{nd})^T \tag{1}$$

where nd denotes the number of design variables, the minimum weight design problem is stated mathematically as minimizing the weight f

$$f(\boldsymbol{b}) = \frac{\rho}{3}\int_\Gamma r_0 \frac{\partial r_0}{\partial n}\, d\Gamma \rightarrow \min \tag{2}$$

subject to the stress constraints

$$g_j(\boldsymbol{b}) = \sigma_j/\sigma_a - 1 \le 0 \qquad (j = 1, 2, \ldots) \tag{3}$$

and the side constraints

$$b_i^L \le b_i \le b_i^U \qquad (i = 1, 2, \ldots, n_d) \tag{4}$$

where n and ρ denote, respectively, the outward unit normal vector to the boundary and the specific gravity of the material, σ_a is an allowable upper limit of the stress at an observation point j, and b_i^L and b_i^U are the lower and upper bounds of the design variable b_i. When an arbitrary point on the boundary is denoted as (x_1, x_2, x_3), r_0 in Eq. (2) indicates a distance from a proper origin (x_1^0, x_2^0, x_3^0) given as

$$r_0^2 = (x_i - x_i^0)(x_i - x_i^0)$$

The repeated index must be summed up in the usual tensor symbolism manner and lower-case Latin indices refer to the Cartesian coordinate directions like $i = 1, 2, 3$ in the following.

Approximate Problem Construction

For solving the minimum weight design problems defined earlier, a mathematical programming method will be used that requires the evaluation of the objective function, the displacement and stress constraint function values, and their sensitivities. It is easy and inexpensive to evaluate the objective function value for the design variable change; however, the structural analysis and its sensitivity analysis have to be done to evaluate the displacement and stress constraints for every design variable change during optimization. Then it is not rare that several hundred times iterations of the structural and sensitivity analyses are required until finally obtaining the optimum shape in the large-scale optimization problems. Therefore, if we can form an approximated problem for which the optimum solution will be searched directly in the approximated design space, it may be expected that the number of the structural and the sensitivity analyses based on the BEM until getting the final solution will be reduced.

For this purpose, a direct approximation to the actual shape optimization problem is constructed by expanding the objective function to a second-order Taylor series at the current design variable $\boldsymbol{b}_0$ as

$$f(\boldsymbol{b}) \cong \tfrac{1}{2}(\boldsymbol{b} - \boldsymbol{b}_0)^T \boldsymbol{C}(\boldsymbol{b} - \boldsymbol{b}_0) + (\nabla f)^T(\boldsymbol{b} - \boldsymbol{b}_0) + f(\boldsymbol{b}_0) \tag{5}$$

and the stress constraints to a first-order Taylor series as

$$g_j(\boldsymbol{b}) \cong (\nabla g_j)^T(\boldsymbol{b} - \boldsymbol{b}_0) + g_j(\boldsymbol{b}_0) \le 0 \tag{6}$$

where

$$\nabla f(\boldsymbol{b}) = \left(\frac{\partial f}{\partial b_1}, \frac{\partial f}{\partial b_2}, \ldots, \frac{\partial f}{\partial b_{nd}}\right)^T$$
$$\nabla g_j(\boldsymbol{b}) = \left(\frac{\partial g_j}{\partial b_1}, \frac{\partial g_j}{\partial b_2}, \ldots, \frac{\partial g_j}{\partial b_{nd}}\right)^T \tag{7}$$

$$\boldsymbol{C} = \begin{bmatrix} \dfrac{\partial^2 f}{\partial b_1^2} & \cdots & \dfrac{\partial^2 f}{\partial b_1 \partial b_{nd}} \\ \cdots & \cdots & \cdots \\ \dfrac{\partial^2 f}{\partial b_{nd} \partial b_1} & \cdots & \dfrac{\partial^2 f}{\partial b_{nd}^2} \end{bmatrix} \tag{8}$$

The evaluation of the first derivative of the constraints requires the displacement and stress sensitivity analyses based on BEM.

The approximated subproblem is solved by a nonlinear programming optimization algorithm with appropriate move limits. The move limits are employed to insure that a new design point remains in the vicinity of the current design point $\boldsymbol{b}_0$ around which the Taylor series was expanded. The move limits are typically specified by a limit factor δ to determine the upper and lower bounds as

$$(1 - \delta)\boldsymbol{b}_0 \le \boldsymbol{b} \le (1 + \delta)\boldsymbol{b}_0, \qquad 0 < \delta < 1 \tag{9}$$

The move limits of Eq. (9) are applied as side constraints instead of Eq. (4), if they are more restrictive than the minimum and maximum gauge constraints.

Design Sensitivity Analysis

Sensitivity of Weight

The first and second derivatives with respect to the design variables are required to construct an approximate objective function (5). When the boundary Γ is discretized into the boundary elements, the coordinate x_i at any point of parametric coordinates (ξ, η) in an element is interpolated by the shape function $N_J(\xi, \eta)$ for node J as

$$x_i = N_J x_{iJ} \tag{10}$$

in which x_{iJ} is a coordinate x_i at the nodal point J in the element, and the upper-case index refers to the nodes in the element. Then, Eq. (2) is discretized as

$$f(\boldsymbol{b}) = \frac{\rho}{3}\sum_e \int_{-1}^{1}\int_{-1}^{1} r_0 \frac{\partial r_0}{\partial n} |J(\xi, \eta)|\, d\xi\, d\eta$$
$$= \frac{\rho}{3}\sum_e \int_{-1}^{1}\int_{-1}^{1} (x_i - x_i^0) n_i |J(\xi, \eta)|\, d\xi\, d\eta \tag{11}$$

where $\sum_e$ means the summation with respect to all boundary elements. When the derivatives with respect to the parametric coordinate ξ, η are expressed as $\partial(\,)/\partial\xi = (\,)_{,\xi}$ and $\partial(\,)/\partial\eta = (\,)_{,\eta}$, the Jacobian determinant and direction cosine n_i in the discretized form are given as

$$|J|^2 = \epsilon_{ijk}\epsilon_{ilm} x_{j,\xi} x_{k,\eta} x_{l,\xi} x_{m,\eta}$$
$$= \epsilon_{ijk}\epsilon_{ilm} N_{I,\xi} N_{J,\eta} N_{K,\xi} N_{L,\eta} x_{jJ} x_{kK} x_{lK} x_{mL}$$
$$n_i = \epsilon_{ijk} x_{j,\xi} x_{k,\eta}/|J| = \epsilon_{ijk} N_{I,\xi} N_{J,\eta} x_{jI} x_{kJ}/|J| \tag{12}$$

in which ϵ_{ijk} denotes a permutation tensor.

Then, differentiating Eq. (11) directly, the first derivative of the objective function with respect to the design parameter b_m is derived as

$$\frac{\partial f}{\partial b_m} = \frac{\rho}{3}\sum_e \int_{-1}^{1}\int_{-1}^{1} \left\{ \left[\frac{\partial x_i}{\partial b_m} n_i + (x_i - x_i^0) \frac{\partial n_i}{\partial b_m} \right] |J| + (x_i - x_i^0) n_i \frac{\partial |J|}{\partial b_m} \right\} d\xi\, d\eta \tag{13}$$

where the derivatives of the Jacobian determinant and the direction cosines are given as

$$|\dot{J}| = \epsilon_{ijk} n_i \left(\frac{\partial x_{j,\xi}}{\partial b_m} x_{k,\eta} + x_{j,\xi} \frac{\partial x_{k,\eta}}{\partial b_m} \right)$$

$$\dot{n}_i = \frac{1}{|J|} \left[\epsilon_{ijk} \left(\frac{\partial x_{j,\xi}}{\partial b_m} x_{k,\eta} + x_{j,\xi} \frac{\partial x_{k,\eta}}{\partial b_m} \right) - n_i n_j \epsilon_{jkl} \left(\frac{\partial x_{k,\xi}}{\partial b_m} x_{l,\eta} + x_{k,\xi} \frac{\partial x_{l,\eta}}{\partial b_m} \right) \right] \tag{14}$$

in which $(\dot{\ }) = \partial(\ )/\partial b_m$. Furthermore, the second derivative of the objective function is also given by the direct differentiation of Eq. (13) with respect to the design parameter b_n as

$$\frac{\partial^2 f}{\partial b_m \partial b_n} = \frac{\rho}{3}\sum_e \int_{-1}^{1}\int_{-1}^{1} \left\{ \left[\frac{\partial^2 x_i}{\partial b_m \partial b_n} n_i + \frac{\partial x_i}{\partial b_m}\frac{\partial n_i}{\partial b_n} + \frac{\partial x_i}{\partial b_n}\frac{\partial n_i}{\partial b_m} + (x_i - x_i^0)\frac{\partial^2 n_i}{\partial b_m \partial b_n} \right] |J| + \left[\frac{\partial x_i}{\partial b_m} n_i + (x_i - x_i^0)\frac{\partial n_i}{\partial b_m} \right] \frac{\partial |J|}{\partial b_n} + \left[\frac{\partial x_i}{\partial b_n} n_i + (x_i - x_i^0)\frac{\partial n_i}{\partial b_n} \right] \frac{\partial |J|}{\partial b_m} + (x_i - x_i^0) n_i \frac{\partial^2 |J|}{\partial b_m \partial b_n} \right\} d\xi\, d\eta \tag{15}$$

The second derivatives of the Jacobian determinant and the direction cosines that are required for the preceding calculation are also given as

$$\frac{\partial^2 |J|}{\partial b_m \partial b_n} = \frac{1}{|J|} \left\{ -\frac{\partial |J|}{\partial b_m}\frac{\partial |J|}{\partial b_n} + \epsilon_{ijk}\epsilon_{ipq} \left[\left(\frac{\partial x_{j,\xi}}{\partial b_m} x_{k,\eta} + x_{j,\xi}\frac{\partial x_{k,\eta}}{\partial b_m} \right) \left(\frac{\partial x_{p,\xi}}{\partial b_n} x_{q,\eta} + x_{p,\xi}\frac{\partial x_{q,\eta}}{\partial b_n} \right) + x_{j,\xi} x_{k,\eta} \left(\frac{\partial x_{p,\xi}}{\partial b_m}\frac{\partial x_{q,\eta}}{\partial b_n} + \frac{\partial x_{p,\xi}}{\partial b_n}\frac{\partial x_{q,\eta}}{\partial b_m} \right) \right] \right\} \tag{16}$$

$$\frac{\partial^2 n_i}{\partial b_m \partial b_n} = \frac{1}{|J|} \left[\epsilon_{ijk} \left(\frac{\partial x_{j,\xi}}{\partial b_m}\frac{\partial x_{k,\eta}}{\partial b_n} + \frac{\partial x_{j,\xi}}{\partial b_n}\frac{\partial x_{k,\eta}}{\partial b_m} \right) - \frac{\partial n_i}{\partial b_m}\frac{\partial |J|}{\partial b_n} - \frac{\partial n_i}{\partial b_n}\frac{\partial |J|}{\partial b_m} - n_i \frac{\partial^2 |J|}{\partial b_m \partial b_n} \right] \tag{17}$$

Displacement Sensitivities Using BEM

The displacement sensitivity is given by solving a system of the boundary element sensitivity equation. When the displacement u_i and the traction p_i at any point in an element are interpolated by the same shape function introduced in Eq. (10) as

$$u_i = N_J u_{iJ}^e, \qquad p_i = N_J p_{iJ}^e \tag{18}$$

where u_{iJ}^e and p_{iJ}^e denote the displacement and traction at node J in the element e, then the discretized boundary integral equation for a source point y_i on the smooth boundary is described as

$$\tfrac{1}{2} u_i(y) + \sum_e \int_{-1}^{1}\int_{-1}^{1} p_{ij}^* N_I u_{jI}^e |J|\, d\xi\, d\eta = \sum_e \int_{-1}^{1}\int_{-1}^{1} u_{ij}^* N_I p_{jI}^e |J|\, d\xi\, d\eta \qquad (i = 1, 2, 3) \tag{19}$$

where u_{ij}^* and p_{ij}^* denote Kelvin's fundamental solutions of the displacement and traction given as

$$u_{ij}^* = \frac{1}{16\pi(1-\nu)\mu r} [(3 - 4\nu)\delta_{ij} + r_{,i} r_{,j}]$$

$$p_{ij}^* = \sigma_{jk}^{*i} n_k = -\frac{1}{8\pi(1-\nu)r^2} \{ [(1 - 2\nu)\delta_{ij} + 3r_{,i} r_{,j}] r_{,n} - (1 - 2\nu)(r_{,i} n_j - r_{,j} n_i) \} \tag{20}$$

$$\sigma_{jk}^{*i} = \frac{1}{8\pi(1-\nu)r^2} [(1 - 2\nu)(\delta_{jk} r_{,i} - \delta_{ij} r_{,k} - \delta_{ik} r_{,j}) - 3r_{,i} r_{,j} r_{,k}]$$

in which μ and ν are the shear modulus and Poisson's ratio; δ_{ij} represents Kronecker's delta, and

$$r^2 = (x_i - y_i)(x_i - y_i), \qquad r_{,i} = (x_i - y_i)/r, \qquad r_{,n} = r_{,i} n_i \tag{21}$$

Differentiating the boundary integral equation (19), the implicit differentiation method leads to the following discretized boundary integral sensitivity equation to be solved for $\dot{u}_{iI}^e = \partial u_{iI}^e/\partial b_m$ and $\dot{p}_{iI}^e = \partial p_{iI}^e/\partial b_m$:

$$\begin{aligned} &\tfrac{1}{2}\dot{u}_i(y) + \sum_e \int_{-1}^{1}\int_{-1}^{1} p_{ij}^* N_I \dot{u}_{jI}^e |J|\, d\xi\, d\eta \\ &\quad + \sum_e \int_{-1}^{1}\int_{-1}^{1} (\dot{p}_{ij}^* |J| + p_{ij}^* |\dot{J}|) N_I u_{jI}^e\, d\xi\, d\eta \\ &\quad = \sum_e \int_{-1}^{1}\int_{-1}^{1} u_{ij}^* N_I \dot{p}_{jI}^e |J|\, d\xi\, d\eta \\ &\quad + \sum_e \int_{-1}^{1}\int_{-1}^{1} (\dot{u}_{ij}^* |J| + u_{ij}^* |\dot{J}|) N_I p_{jI}^e\, d\xi\, d\eta \\ &\qquad\qquad (i = 1, 2, 3) \end{aligned} \tag{22}$$

The derivatives of the fundamental solution that appear in the preceding equation are calculated from

$$\dot{u}_{ij}^* = u_{ij,k}^* \left(\frac{\partial x_k}{\partial b_m} - \frac{\partial y_k}{\partial b_m} \right)$$

$$u_{ij,k}^* = \frac{1}{16\pi(1-\nu)\mu r^2} [-(3 - 4\nu)\delta_{ij} r_{,k} + \delta_{ik} r_{,j} + \delta_{jk} r_{,i} - 3r_{,i} r_{,j} r_{,k}]$$

$$\dot{p}_{ij}^* = \sigma_{jk,l}^{*i} \left(\frac{\partial x_l}{\partial b_m} - \frac{\partial y_l}{\partial b_m} \right) n_k + \sigma_{jk}^{*i} \dot{n}_k \tag{23}$$

$$\sigma_{jk,l}^{*i} n_k = -\frac{1}{8\pi(1-\nu)r^3} \{ (1 - 2\nu)(\delta_{ij} n_l + \delta_{jl} n_i - \delta_{il} n_j + 3r_{,i} r_{,l} n_j - 3r_{,j} r_{,l} n_i) + 3r_{,i} r_{,j} n_l - 3[(1 - 2\nu)\delta_{ij} r_{,l} - \delta_{il} r_{,j} - \delta_{jl} r_{,i} + 5r_{,i} r_{,j} r_{,l}] r_{,k} n_k \}$$

A square system of algebraic equations for the sensitivities of the surface displacement and traction is obtained by locat-

ing the source point y of Eq. (22) at every node on the boundary:

$$[H]\{\dot{U}\} + [\dot{H}]\{U\} = [G]\{\dot{P}\} + [\dot{G}]\{P\} \tag{24}$$

where $[H]$ and $[G]$ denote the usual coefficient matrices of the system of boundary integral equations (19) that correspond to the first and second terms of the left-hand side and the first term of the right-hand side of Eq. (22), and $\{U\}$ and $\{P\}$ are column vectors of displacement and traction components of all nodes. A rigid-body integral identity is used to remove singularities that arise when taking derivatives of the basic Kelvin's kernels. If the coefficient matrix of Eq. (19) after processing the boundary conditions has been decomposed like LU and the solution of $\{U\}$ and $\{P\}$ have been obtained, we can solve the previous equation for the displacement and traction sensitivities by forming only the terms of $[\dot{H}]\{U\}$ and $[\dot{G}]\{P\}$.

Boundary Stresses and Their Sensitivities

The stress sensitivity is also required to construct approximate stress constraints of Eq. (6). The sensitivities of stress components are also calculated from the derivative form of the stress recovery equation at each boundary node. The displacement gradients with respect to the coordinates are usually obtained by solving the following relations:

$$\begin{bmatrix} \mu(n_2^2+n_3^2)+an_1^2 & (\mu+\lambda)n_1^2 & (\mu+\lambda)n_1^2 \\ (\mu+\lambda)n_2^2 & \mu(n_3^2+n_1^2)+an_2^2 & (\mu+\lambda)n_2^2 \\ (\mu+\lambda)n_3^2 & (\mu+\lambda)n_3^2 & \mu(n_1^2+n_2^2)+an_3^2 \end{bmatrix} \begin{bmatrix} u_{1,1} \\ u_{2,2} \\ u_{3,3} \end{bmatrix}$$

$$= \begin{bmatrix} p_1n_1 - \mu(u_{12}^t n_3 - u_{13}^t n_2 + u_{23}^t n_1 - u_{32}^t n_1) \\ p_2n_2 - \mu(u_{23}^t n_1 - u_{21}^t n_3 + u_{31}^t n_2 - u_{13}^t n_2) \\ p_3n_3 - \mu(u_{31}^t n_2 - u_{32}^t n_1 + u_{12}^t n_3 - u_{21}^t n_3) \end{bmatrix} \tag{25}$$

$$(u_{1,2}+u_{2,1})n_1n_2 = u_{23}^t n_1 - u_{13}^t n_2 + u_{1,1}n_2^2 + u_{2,2}n_1^2$$
$$(u_{2,3}+u_{3,2})n_2n_3 = u_{31}^t n_2 - u_{21}^t n_3 + u_{2,2}n_3^2 + u_{3,3}n_2^2$$
$$(u_{3,1}+u_{1,3})n_3n_1 = u_{12}^t n_3 - u_{32}^t n_1 + u_{3,3}n_1^2 + u_{1,1}n_3^2$$

where $\lambda = 2\mu\nu/(1-2\nu)$, $a = 2\mu + \lambda$, and u_{ij}^t denotes the displacement gradient of u_i in the tangential direction to the boundary defined as

$$u_{ij}^t = (u_{i,\eta}x_{j,\xi} - u_{i,\xi}x_{j,\eta})/|J| \qquad (i \neq j)$$

Then the stress recovery equation is given as

$$\sigma_{ij} = \lambda\delta_{ij}u_{k,k} + \mu(u_{i,j} + u_{j,i}) \tag{26}$$

By differentiating Eqs. (25) directly, we will get the sensitivity equations to calculate the sensitivities of the displacement gradients by using the displacement sensitivities obtained from Eq. (24):

$$\begin{bmatrix} \mu(n_2^2+n_3^2)+an_1^2 & (\mu+\lambda)n_1^2 & (\mu+\lambda)n_1^2 \\ (\mu+\lambda)n_2^2 & \mu(n_3^2+n_1^2)+an_2^2 & (\mu+\lambda)n_2^2 \\ (\mu+\lambda)n_3^2 & (\mu+\lambda)n_3^2 & \mu(n_1^2+n_2^2)+an_3^2 \end{bmatrix} \begin{bmatrix} \dot{u}_{1,1} \\ \dot{u}_{2,2} \\ \dot{u}_{3,3} \end{bmatrix}$$

$$= \begin{bmatrix} \dot{p}_1n_1 + p_1\dot{n}_1 - \mu(\dot{u}_{12}^t n_3 + u_{12}^t\dot{n}_3 - \dot{u}_{13}^t n_2 - u_{13}^t\dot{n}_2 + \dot{u}_{23}^t n_1 + u_{23}^t\dot{n}_1 - \dot{u}_{32}^t n_1 - u_{32}^t\dot{n}_1) \\ \dot{p}_2n_2 + p_2\dot{n}_2 - \mu(\dot{u}_{23}^t n_1 + u_{23}^t\dot{n}_1 - \dot{u}_{21}^t n_3 - u_{21}^t\dot{n}_3 + \dot{u}_{31}^t n_2 + u_{31}^t\dot{n}_2 - \dot{u}_{13}^t n_2 - u_{13}^t\dot{n}_2) \\ \dot{p}_3n_3 + p_3\dot{n}_3 - \mu(\dot{u}_{31}^t n_2 + u_{31}^t\dot{n}_2 - \dot{u}_{32}^t n_1 - u_{32}^t\dot{n}_1 + \dot{u}_{12}^t n_3 + u_{12}^t\dot{n}_3 - \dot{u}_{21}^t n_3 - u_{21}^t\dot{n}_3) \end{bmatrix}$$

$$- 2\begin{bmatrix} \mu(n_2\dot{n}_2 + n_3\dot{n}_3) + an_1\dot{n}_1 & (\mu+\lambda)n_1\dot{n}_1 & (\mu+\lambda)n_1\dot{n}_1 \\ (\mu+\lambda)n_2\dot{n}_2 & \mu(n_3\dot{n}_3 + n_1\dot{n}_1) + an_2\dot{n}_2 & (\mu+\lambda)n_2\dot{n}_2 \\ (\mu+\lambda)n_3\dot{n}_3 & (\mu+\lambda)n_3\dot{n}_3 & \mu(n_1\dot{n}_1 + n_2\dot{n}_2) + an_3\dot{n}_3 \end{bmatrix} \begin{bmatrix} u_{1,1} \\ u_{2,2} \\ u_{3,3} \end{bmatrix}$$

$$(\dot{u}_{1,2}+\dot{u}_{2,1})n_1n_2 = \dot{u}_{23}^t n_1 - \dot{u}_{13}^t n_2 + u_{23}^t\dot{n}_1 - u_{13}^t\dot{n}_2 + \dot{u}_{1,1}n_2^2 + \dot{u}_{2,2}n_1^2 + 2u_{1,1}n_2\dot{n}_2 + 2u_{2,2}n_1\dot{n}_1 - (u_{1,2}+u_{2,1})(\dot{n}_1n_2 + n_1\dot{n}_2)$$
$$(\dot{u}_{2,3}+\dot{u}_{3,2})n_2n_3 = \dot{u}_{21}^t n_2 - \dot{u}_{21}^t n_3 + u_{31}^t\dot{n}_2 - u_{21}^t\dot{n}_3 + \dot{u}_{2,2}n_3^2 + \dot{u}_{3,3}n_2^2 + 2u_{2,2}n_3\dot{n}_3 + 2u_{3,3}n_2\dot{n}_2 - (u_{2,3}+u_{3,2})(\dot{n}_2n_3 + n_2\dot{n}_3) \tag{27}$$
$$(\dot{u}_{3,1}+\dot{u}_{1,3})n_3n_1 = \dot{u}_{12}^t n_3 - \dot{u}_{32}^t n_1 + u_{12}^t\dot{n}_3 - u_{32}^t\dot{n}_1 + \dot{u}_{3,3}n_1^2 + \dot{u}_{1,1}n_3^2 + 2u_{3,3}n_1\dot{n}_1 + 2u_{1,1}n_3\dot{n}_3 - (u_{3,1}+u_{1,3})(\dot{n}_3n_1 + n_3\dot{n}_1)$$

where

$$\dot{u}_{ij}^t = (\dot{u}_{i,\eta}x_{j,\xi} + u_{i,\eta}\dot{x}_{j,\xi} - \dot{u}_{i,\xi}x_{j,\eta} - u_{i,\xi}\dot{x}_{j,\eta} - u_{ij}^t|\dot{J}|)/|J| \qquad (i \neq j)$$

The right-hand side of the preceding equation can be evaluated from the sensitivities of displacements, and the gradient sensitivities of Eqs. (27) are solved easily. Then the stress sensitivities on the boundary can be obtained from

$$\dot{\sigma}_{ij} = \lambda\delta_{ij}\dot{u}_{k,k} + \mu(\dot{u}_{i,j} + \dot{u}_{j,i}) \tag{28}$$

Design Variable Reduction and Adaptive Remeshing

To achieve the effective implementation of shape optimization, it is important to reduce the number of the design variables as much as possible. There are two common ways to represent a boundary shape of a solid model, i.e., the constructive solid geometry (CSG) scheme[18] and the boundary representation (B-Rep) scheme. In the B-Rep scheme, the boundary shape is defined and controlled directly by the design variables, where the representative values to define individual points, curves, and surface or coefficients of trigonometric series and the Fourier series are taken as the design variables.[19,20] This scheme achieves intuitive control of boundary shape, whereas it requires direct definition of the relationship between the design variables and the boundary nodes by the program or the input data to implement the sensitivity analysis and the adaptive remeshing, and the process makes the implementation difficult for the three-dimensional shape optimization using the finite element method. On the other hand, the CSG approach uses the geometric modeling scheme and constructs the geometry by the operation of basic primitives, and then the mesh is generated automatically. This approach enables us to take any parameters to define the basic primitives as the design variables and provides the practical design-oriented manner for the shape optimization. However, the CSG approach requires the solid modeler and the automatic mesh generator. Therefore, the B-Rep scheme is adopted in this study for simplicity because the boundary element analysis requires subdivision of the model surface only.

The adaptive remeshing technique is also important to avoid the warped boundary element due to the large variation of the design variables. The discrete transfinite mapping technique,[21] which can treat the discrete information of the subboundary and correlate the boundary information to the interior mesh very well, is employed when the edge shape of the boundary surface is complex and relates to several design variables; otherwise the boundary node position on the surface is defined by the design variable directly. When u and v denote the parametric coordinates in a subsurface ($0 \le u, v \le 1$) and the edge shapes $\phi_1(u)$, $\phi_2(u)$, $\varphi_1(v)$, and $\varphi_2(v)$ are given as shown

in Fig. 2, the discrete transfinite mapping provides the coordinates x_i of interior node (u, v) on the subsurface as

$$x_i(u, v) = (1 - v)\varphi_1(u) + v\varphi_2(u) + (1 - u)\phi_1(v) + u\phi_2(v) - (1 - u)(1 - v)x_i(0, 0) - (1 - u)vx_i(0, 1) - uvx_i(1, 1) - u(1 - v)x_i(1, 0) \quad (29)$$

where $x_i(0, 0)$, $x_i(0, 1)$, $x_i(1, 0)$, and $x_i(1, 1)$ denote the coordinates of vertices of the quadrilateral subsurface. After the node positions on the edge of the subsurface are defined by the design variables, the interior node positions are calculated by Eq. (29).

Numerical Examples

A computer program to calculate the displacement and stress sensitivities is coded for the quadratic isoparametric element with eight nodes and applied to the three-dimensional shape optimization of typical design models. The complementary pivot method[22] is adopted as a practical sequential quadratic programming method for optimization.

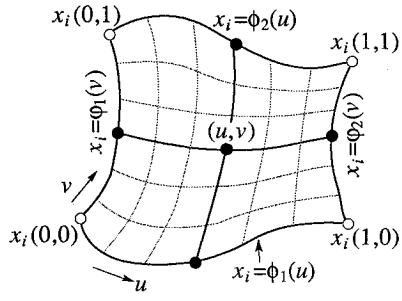

Fig. 2 Discrete transfinite mapping.[21]

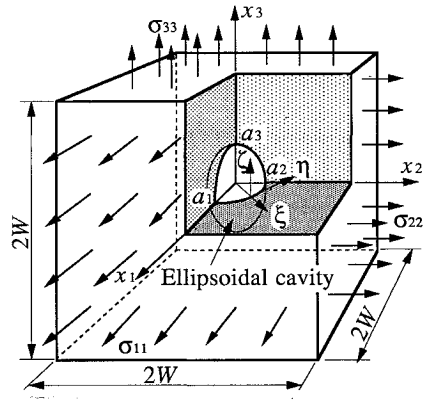

Fig. 3 Elastic cube with an ellipsoidal cavity under triaxial uniform tension loading.

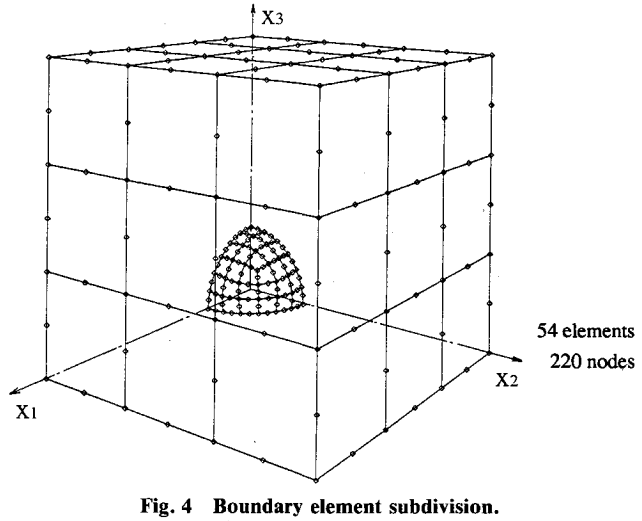

Fig. 4 Boundary element subdivision.

Table 1 Comparison of stress sensitivities [$\Delta a_1/a_1 = \Delta a_3/a_3 = 0.01$, $R = (a_1 + a_2 + a_3)/3$]

$a_3/a_1 = a_3/a_2$		0.5	1.0	2.0
$(\partial\sigma_{\eta\eta}/\partial a_1)R/\sigma_0$	BEM[a]	0.9784	1.320	3.113
at $x_1 = a_1$	SAM[b]	0.9559	1.300	3.084
$(\partial\sigma_{\eta\eta}/\partial a_3)R/\sigma_0$	BEM	−2.974	−0.0988	−0.4063
at $x_1 = a_1$	SAM	−2.882	−0.0728	−0.4426
$(\partial\sigma_{\zeta\zeta}/\partial a_1)R/\sigma_0$	BEM	3.524	2.148	1.791
at $x_1 = a_1$	SAM	3.448	2.106	1.767
$(\partial\sigma_{\zeta\zeta}/\partial a_3)R/\sigma_0$	BEM	−15.06	−4.112	−1.322
at $x_1 = a_1$	SAM	−14.71	−3.993	−1.343
$(\partial\sigma_{\eta\eta}/\partial a_1)R/\sigma_0$	BEM	−0.8599	−1.857	−3.450
at $x_3 = a_3$	SAM	−0.8563	−1.858	−3.608
$(\partial\sigma_{\eta\eta}/\partial a_3)R/\sigma_0$	BEM	1.948	1.100	−6.057
at $x_3 = a_3$	SAM	1.931	1.082	−6.113

[a]BEM: implicit differentiation method.
[b]SAM: semianalytical method.

Ellipsoidal Cavity Shape in a Cube Under Triaxial Uniform Tension

In the first example, a cube of side length $2W$ with an ellipsoidal cavity of semiaxes a_1, a_2, a_3 under uniform tension loadings $2\sigma_0$, $2\sigma_0$, $3\sigma_0$ in the x_1, x_2, x_3 directions is considered as shown in Fig. 3. The mechanical properties of Young's modulus and Poisson's ratio are assumed to be $E = 205.8$ GPa and $\nu = 0.3$. Because of symmetry, quadrant boundaries of the model are discretized into 54 quadratic elements and 220 nodes, and 27 elements with 100 nodes cover the ellipsoidal boundary as shown in Fig. 4. The cavity shape is interpolated by the trigonometric interpolating function in the first quadrant as

$$x_1 = a_1\cos\varphi\cos\theta, \qquad x_2 = a_2\sin\varphi\cos\theta$$
$$x_3 = a_3\sin\theta \qquad (0 \le \theta, \varphi \le \pi/2) \quad (30)$$

where θ and φ are the angles of latitude and longitude, and the major axes $a_1 = a_2$ and a_3 are selected as the design variables. If more precise determination of cavity shape is required, two or more terms of the trigonometric series or Fourier series functions discussed in Refs. 19 and 20 should be adopted to represent the boundary shape of the cavity.

Table 1 shows the sensitivities of tangential stress $\sigma_{\eta\eta}$ and meridional stress $\sigma_{\zeta\zeta}$ with respect to the shape parameters $a_1 = a_2$ and a_3 at the cavity boundary in comparison with the corresponding values by the semianalytic method, in which the derivatives of the coefficient matrices $[H]$ and $[G]$ are calculated by the finite difference method and solved the assembled system of Eq. (24) analytically, when the ratio $a_3/a_1 = 0.5$, 1.0, and 2.0 with keeping $a_1/W = a_2/W = 0.25$. In the semianalytic method, the central difference and the perturbation $\Delta a_1/a_1 = \Delta a_2/a_2 = \Delta a_3/a_3 = 0.01$ are used. Both sensitivity values coincide with each other. The computer time to calculate the sensitivities by the implicit differentiation method formulated here is less than one-third of the time by the semianalytic method.

The minimum weight design of the ellipsoidal cavity shape subject to the stress constraints is implemented by using the sensitivity analysis technique of the implicit differentiation method. The Von Mises stress values on the ellipsoidal cavity boundary are restricted less than the allowable stress $\sigma_a = 4.0\sigma_0$, and the stress constraints are imposed at several points on the ellipsoidal boundary. The optimum solutions of the design variables, the objective function, and the stress constraints at $\theta = 0$ deg (g_3), 45 deg (g_2), and 90 deg (g_1) along the meridian obtained after six iterations of optimization are tabulated in Table 2 in comparison with the initial values. The

Table 2 Comparison of objective function, stress constraint, and design variables

	Initial	Optimum without lower bound	Optimum with lower bound
a_1/W	0.250	0.440	0.380
a_3/W	0.250	0.679	0.804
f/W^3	0.992	0.931	0.933
g_1	−0.425	−0.244	−0.075
g_2	−0.164	-0.227×10^{-8}	-0.330×10^{-9}
g_3	0.123	0.368×10^{-13}	−0.0615
g_4	−0.214	—	−0.0146
g_5	0.378	—	-0.384×10^{-13}

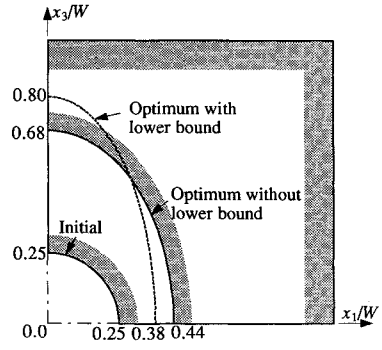

Fig. 5 Initial and optimum shapes.

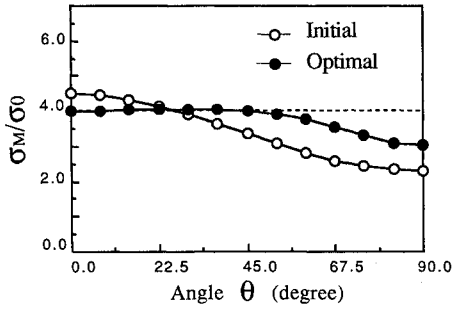

Fig. 6 Distributions of the Von Mises stress along the meridian of an ellipsoidal cavity.

stress constraints at $\theta = 0$ and 45 deg are active in the optimum shape. The solid lines in Fig. 5 show the initial and optimum shapes with the upper bound of stress constraints. The stress distributions of the initial and optimum shapes along the meridian of the ellipsoid are shown in Fig. 6. If the cavity that exists in the infinite body applied the same uniform tension at infinity, the elastic theory gives an optimum ellipsoid with the ratio $a_3/a_1 = 2.0$, which has the uniform distributions of all principal stresses along the cavity boundary.[23] The optimum shape obtained here, however, does not give the uniform distribution because of the existence of the outer boundary. To confirm this fact, the optimum shape that has more uniform stress distribution along the cavity boundary is searched by adding the lower bound constraints of the Von Mises stress as

$$g_j = 1 - \sigma_j/3.7\sigma_0 \leq 0 \tag{31}$$

The broken line in Fig. 5 shows the optimum shape for the preceding constraints in which the upper bound constraint $g_2(\theta = 45 \text{ deg})$ and the lower bound constraints $g_4(\theta = 0 \text{ deg})$ and $g_5(\theta = 90 \text{ deg})$ are active. The optimum solution is also tabulated in Table 2. The other solution with more severe lower bound is also tried to search; however, it failed to find the admissible design point. The solution with the constraint of Eq. (31) gives better stress distribution than the shape with only the upper bound constraints, although its volume is about 9% greater. Finally, it is confirmed that the optimum shape shown by the solid line in Fig. 5 is the real solution for the stress constraints considered here.

Connecting Rod Under Axial Compression

Next, the shape design of a rod connecting the piston with the crankshaft of an internal combustion engine is considered as shown in Fig. 7. The outer radii of big and small ends, the rod width, and the root radii between the rod and the outer surface of both ends are taken as the design variables. The high strength aluminum alloy is assumed, i.e., $E = 70.56$ GPa, $\nu = 0.3$. The compressive pressure, the maximum value of which is $p_{max} = 52.1$ MPa at the small end, is applied on a half-region of the inner surface of both ends as contact pressure with trigonometric distribution corresponding to the maximum explosive load. The allowable stress limit is taken as $\sigma_a = 3\,p_{max} = 156.4$ MPa, and the Von Mises stress values are restricted at the inner surface of both ends, the root surface between the rod and the outer surface of both ends, and the central part of the rod surface. The adaptive remeshing technique is employed for all regions of the model to avoid the warped boundary element due to the large variation of the design variables. In particular, a discrete transfinite mapping technique is applied to the shaded regions, including connecting parts between the rod and both ends as shown in Fig. 8. The initial values of the design variables are taken as $b_1 = 31.5$, $b_2 = 10.0$, $b_3 = 60.0$, $b_4 = 17.0$, and $b_5 = 40.0$ (in

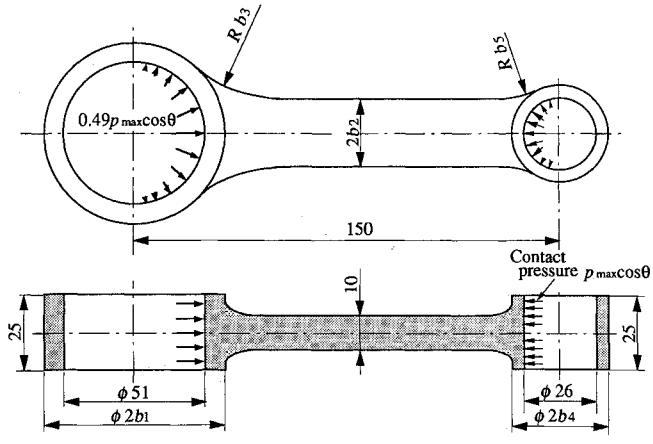

Fig. 7 Design model of a connecting rod under axial compression.

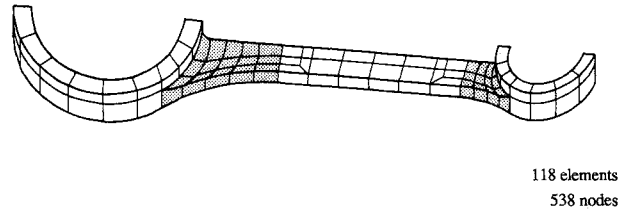

Fig. 8 Boundary element subdivision of a connecting rod.

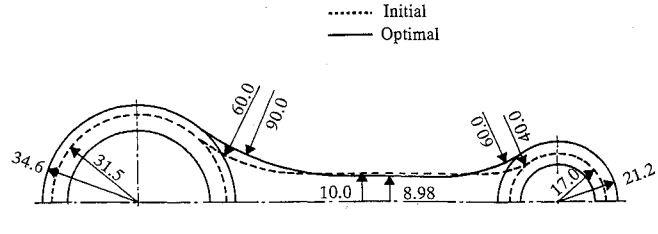

Fig. 9 Initial and optimum shapes of a connecting rod.

Table 3 Comparison of objective function, stress constraints, and design variables

	Initial	Optimal
Objective function f/f_0	1.000	1.467
Design variable, mm		
b_1	31.50	34.57
b_2	10.00	8.979
b_3	60.00	90.00
b_4	17.00	21.21
b_5	40.00	60.00
Constraint		
g_1	0.159	-0.117
g_2	0.917	-0.367×10^{-2}
g_3	-0.151	-0.057
g_4	0.760	1.699×10^{-5}
g_5	0.677	-6.796×10^{-5}

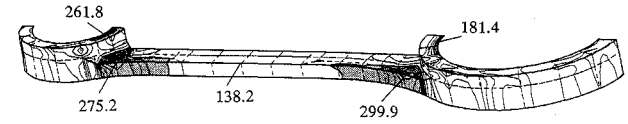

a) Initial shape

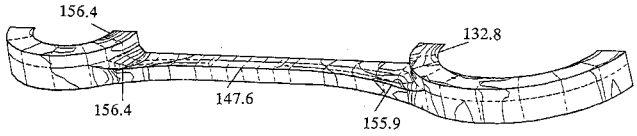

b) Optimum shape

Fig. 10 Von Mises stress distributions along the boundary surface of a connecting rod.

millimeters), and the upper and lower bounds are restricted from the geometric constraints (in millimeters) as

$$b_1 \geq 26.5, \quad 10.0 \geq b_2 \geq 5.0, \quad b_3 \leq 90.0, \quad b_4 \geq 14.0, \quad b_5 \leq 60.0$$

The values of the objective function, the stress constraints, and the design variables of the optimum shape obtained after four iterations of optimization are tabulated in Table 3 in comparison with the initial values, where f_0 is the initial weight. In the optimum solution, every design variable except b_2 becomes larger than the initial value, and the upper bounds of the design variables, b_3 and b_5, and three stress constraints are active. The initial and optimum shapes are shown in Fig. 9. The Von Mises stress distributions along the edge of boundary surfaces for the initial and optimum shapes are shown in Fig. 10. The Von Mises stress concentration at the root surface and the inner surface of both ends in the initial shape is reduced to the allowable value in the optimum shape.

Conclusions

A practical design sensitivity calculation technique of displacements and stresses for three-dimensional bodies based on the implicit differentiation method of discrete integral equations using the boundary element method as well as the weight sensitivities is formulated. A shape optimization technique using the approximation method based on the boundary element sensitivity analysis is suggested for the minimum weight design problem of three-dimensional bodies under stress constraints. The technique was applied to determine an ellipsoidal cavity shape in a cube under triaxial uniform tension and the boundary shape of a connecting rod under axial compression. From these numerical results, it is confirmed that the technique suggested here can treat the large design variable change with the aid of the adaptive remeshing technique and can search the optimum solution effectively.

References

[1]Mota Soares, C. A., Rodrigues, H. C., and Choi, K. K., "Shape Optimal Structural Design Using Boundary Elements and Minimum Compliance Techniques," *Transactions of ASME, Journal of Mechanisms, Transmissions, and Automations in Design,* Vol. 106, No. 4, 1984, pp. 518–523.

[2]Choi, J. H., and Kwak, B. M., "Boundary Integral Equation Method for Shape Optimization of Elastic Structures," *International Journal for Numerical Methods in Engineering,* Vol. 26, No. 7, 1988, pp. 1579–1595.

[3]Sandgren, E., and Wu, S. J., "Shape Optimization Using the Boundary Element Method with Substructuring," *International Journal for Numerical Methods in Engineering,* Vol. 26, No. 9, 1988, pp. 1913–1924.

[4]Meric, R. A., "Shape Design Sensitivity Analysis for Non-Linear Anisotropic Heat Conducting Solids and Shape Optimization by the BEM," *International Journal for Numerical Methods in Engineering,* Vol. 26, No. 1, 1988, pp. 109–120.

[5]Hajela, P., and Jih, J., "Adaptive Grid Refinement in a BEM-Based Optimal Shape Synthesis," *International Journal of Solids and Structures,* Vol. 26, No. 1, 1990, pp. 29–41.

[6]Yang, R. J., "Component Shape Optimization Using BEM," *Computers and Structures,* Vol. 37, No. 4, 1990, pp. 561–568.

[7]Barone, M. R., and Yang, R. J., "Boundary Integral Equations for Recovery of Design Sensitivities in Shape Optimization," *AIAA Journal,* Vol. 26, No. 5, 1988, pp. 589–594.

[8]Kane, J. H., and Saigal, S., "Design Sensitivity Analysis of Solids Using BEM," *Transactions of ASCE, Journal of Engineering Mechanics,* Vol. 114, No. 10, 1988, pp. 1703–1722.

[9]Barone, M. R., and Yang, R. J., "A Boundary Element Approach for Recovery of Shape Sensitivities in Three-Dimensional Elastic Solids," *Computational Methods in Applied Mechanics and Engineering,* Vol. 74, No. 1, 1989, pp. 69–82.

[10]Choi, J. H., and Choi, K. K., "Direct Differentiation Method for Shape Design Sensitivity Analysis Using Boundary Integral Formulation," *Computers and Structures,* Vol. 34, No. 3, 1990, pp. 499–508.

[11]Saigal, S., and Kane, J. H., "Design Sensitivity Analysis of Boundary Element Substructures," *AIAA Journal,* Vol. 28, No. 7, 1990, pp. 1277–1284.

[12]Schmit, L. A., and Miura, H., "Approximation Concepts for Efficient Structural Synthesis," NASA CR-2552, 1976.

[13]Starnes, J. H., and Haftka, R. T., "Preliminary Design of Composite Wings for Buckling, Strength and Displacement Constraints," *Journal of Aircraft,* Vol. 16, No. 8, 1976, pp. 564–570.

[14]Fleury, C., and Braibant, V., "Structural Optimization—A New Dual Method Using Mixed Variables," *International Journal for Numerical Methods in Engineering,* Vol. 23, No. 3, 1986, pp. 409–428.

[15]Vanderplaats, G. N., and Salajegheh, V. A., "A New Approximation Method for Stress Constraints in Structural Synthesis," *AIAA Journal,* Vol. 27, No. 3, 1989, pp. 352–358.

[16]Yang, R. J., and Botkin, M. E., "A Modular Approach for Three-Dimensional Shape Optimization of Structures," *AIAA Journal,* Vol. 25, No. 3, 1987, pp. 492–497.

[17]Kodiyalam, S., and Vanderplaats, G. N., "Shape Optimization of Three-Dimensional Continuum Structures via Force Approximation Techniques," *AIAA Journal,* Vol. 27, No. 9, 1989, pp. 1256–1263.

[18]Kodiyalam, S., Kumar, V., and Finnigan, P. M., "Constructive Solid Geometry Approach to Three-Dimensional Structural Shape Optimization," *AIAA Journal,* Vol. 30, No. 5, 1992, pp. 1408–1415.

[19]Kodiyalam, S., Vanderplaats, G.N., and Miura, H., "Structural Shape Optimization with MSC/NASTRAN," *Computers and Structures,* Vol. 40, No. 4, 1991, pp. 821–829.

[20]Yamazaki, K., Sakamoto, J., and Kitano, M., "An Efficient Shape Optimization Technique of a Two-Dimensional Body Based on the Boundary Element Method," *Computers and Structures,* Vol. 48, No. 6, 1993, pp. 1073–1081.

[21]Haber, R., Shephard, M. S., Abel, J. F., Gallagher, R. H., and Greenberg, D. P., "A General Two-Dimensional Graphical Finite Element Preprocessor Utilizing Discrete Transfinite Mappings," *International Journal for Numerical Methods in Engineering,* Vol. 17, No. 7, 1981, pp. 1015–1044.

[22]Bazaraa, M. S., and Shetty, C. M., *Nonlinear Programming, Theory and Algorithms,* Wiley, New York, 1973, pp. 437–453.

[23]Yamazaki, K., and Oda, J., "Optimum Shape of Elastic Inclusion in Infinite Elastic Solid Under Triaxial Stress Field," *Proceedings of International Conference on Computational Mechanics,* Springer-Verlag, Tokyo, 1986, pp. 83–89.